QUANTITATIVE CHARACTERIZATION OF DENSE BODY, AUTOPHAGIC VACUOLE, AND ACID PHOSPHATASE-BEARING PARTICLE POPULATIONS DURING THE EARLY PHASES OF GLUCAGON-INDUCED AUTOPHAGY IN RAT LIVER

RUSSELL L. DETER

From the Department of Anatomy, Baylor College of Medicine, Houston, Texas 77025

ABSTRACT

Quantitative characterization of dense body, autophagic vacuole and acid phosphatase–bearing particle populations of rat liver have been made at 10 min intervals during the first 50 min following the intraperitoneal administration of glucagon. Beginning 10 to 20 min postinjection, increases in the number of autophagic vacuoles and in the osmotic sensitivity of acid phosphatase–bearing particles were observed, associated with a progressive disappearance of dense bodies. These changes appeared to reach a maximum 50 min after treatment. The average volume of autophagic vacuoles was found to be 440–870% greater than that of normal dense bodies during this time period. No consistent change in total acid phosphatase activity was noted. A detailed study of autophagic vacuole profile populations revealed the presence of five different types of profiles, two of which, types I and II, accounted for 76.3–94.4% of the profiles examined. Type I profiles primarily contained elements of the endoplasmic reticulum, free ribosomes, and ground cytoplasm. Type II profiles had mitochondrial profiles as their principal constituent, but endoplasmic reticulum and free ribosomes were also seen. At all time points type I profiles predominated, comprising 55–69% of the profiles found. Both profile types were bounded by single and double limiting membranes, the former being predominate. A time-dependent change in the ratio of single to double membrane–limited profiles could not be demonstrated. Morphometric parameters derived from profile size distributions indicated that the number of types I and II autophagic vacuoles increased with time, the rate being greater for the type II particle, except between 40 and 50 min. The average volume of the type II autophagic vacuole was consistently greater than that of the type I.

INTRODUCTION

Glucagon-induced autophagy in rat liver, a model of the autophagic process observed in a wide variety of normal and experimental situations (see Ericsson (1) for a review), has been the subject of a number of recent investigations (2–5, 20). These studies have revealed that glucagon stimulates the sequestration of cytoplasmic constituents within vacuoles which appear to be derived from elements of the smooth endoplasmic reticulum and in which subsequent digestion by acid

hydrolases occurs. The enzymes and membranes participating in these events seem to be those formed prior to induction of the autophagic process.

While general agreement has been reached on the basic outlines of the autophagic process provoked by glucagon, a difference of opinion exists concerning the principal source of the acid hydrolases found in autophagic vacuoles. Deter et al. (3) concluded, on the basis of changes in the physical properties of particles containing acid hydrolases and morphometric parameters of autophagic vacuole and pericanalicular dense body populations, that preexisting dense bodies provide most of these degradative enzymes. This concept has been supported by Ericsson (5) who demonstrated the presence of iron particles in autophagic vacuoles found in the livers of glucagon-treated animals whose secondary lysosomes (i.e. dense bodies, telolysosomes) had been preloaded with an iron–sorbitol–citric acid complex. Arstila and Trump (4), however, have stated that Golgi vesicles rather than secondary lysosomes are the principal source of these enzymes, on the basis of a combined biochemical, cytochemical, and morphological study of glucagon-induced autophagy in rat liver. This conclusion will be discussed more fully in the Discussion.

To examine more closely the relationship of preexisting lysosomes to the autophagic process induced by glucagon, a quantitative morphological study of dense body and autophagic vacuole populations during the first 50 min following glucagon injection was undertaken. Observed changes were correlated with alterations in the osmotic sensitivity of particles containing acid phosphatase. Because of the quantitative nature of the morphological data obtained, a more complete description of autophagic vacuole populations during different phases of the autophagic response has been possible.

METHODS

The biochemical and morphological procedures used in these experiments are similar to those previously described (2, 3). 200–250 g male Sprague-Dawley rats were fasted for 12–14 hr, injected intraperitoneally with 50 μg/100 g body weight of crystalline glucagon (Eli Lilly & Co., Indiannapolis, Ind.) in glycine buffer, or glycine buffer alone, and killed by decapitation at 10 min intervals between 0 and 50 min. Two animals receiving buffer and three or four receiving glucagon were studied at each time point. Following decapitation, the livers of these animals were excised, weighed, homogenized in 0.25 M sucrose, and separated into nuclear fractions (N) and cytoplasmic extracts (6). The cytoplasmic extracts (E) were further subdivided into M + L and P + S fractions by differential centrifugation. A single centrifugation of 307,500g · min in a Beckman L2-65B ultracentifuge with a Type 65 rotor effected these separations (Beckman Instruments, Inc., Fullerton, Calif.). Determination of the total acid phosphatase (β-glycerophosphate phosphohydrolase) activity in each of the four isolated fractions, together with an evaluation of the osmotic fragility of particles bearing this enzyme in the E, M + L, and P + S fractions, was carried out as previously described (2).

Morphological studies were confined to the M + L fractions studied biochemically. Pellets prepared by the filtration method of Baudhuin et al. (7) were sectioned and the sections were placed on 300 mesh bar grids. Following staining (8, 9), these sections were examined at 100 kv in an RCA EMU-3G electron microscope. A series of micrographs were made from each preparation with a specially constructed 70 mm roll film camera (10) having a 400 negative capacity. A rotating specimen holder (Fullam Co., Schenectady, N.Y.) was used to align the long axis of the pellet with that of the film. This permitted as many as 20 negatives to be made with a single setting of the illumination and focus.

Errors due to variations in microscope magnification and distortion were evaluated by means of a calibrated grating replica (Fullam Co., Schenectady, N.Y.) having 28,800 lines per inch. Preliminary studies indicated that magnification variation from all causes was 0.80 $\pm$ 0.56 SD %, and distortion 0.70 $\pm$ 0.46 SD % at the approximately 4000 magnification used. A final print magnification of 15,650 $\pm$ 136 SD for all micrographs was obtained by photographing the grating replica before each series of micrographs was made, matching this replica negative to a print of the replica of known magnification, and printing the subsequent negatives of the series without changing conditions except for focusing. A second replica negative was made at the end of most series and was found to differ from the first by 1.38 $\pm$ 1.3 SD %.

Morphometric parameters for dense body and autophagic vacuole populations were determined by the methods described by Baudhuin and Berthet (11) and Baudhuin (12). Profile size distributions for these two types of particles were obtained with a Zeiss TGZ3 (Carl Zeiss, Inc., New York) particle size analyzer, at least 100 profiles being measured in almost all cases. Identification of the profile type and its boundary was facilitated by the use of a 3 diopter viewing lens (Dazor Mfg. Corp., St. Louis, Mo.). Morphometric characteristics of the two particle classes were calculated from profile size distributions

TABLE I

Distribution of Acid Phosphatase in Fractions

Values given are means calculated from data obtained from either two (control) or four (glucagon) animals. Results were analyzed statistically by 2 × 2 × 6 factorial variance analysis. Pairs of means at each time point were compared by *t* tests.

Time after treatment	Treatment	Absolute values N + E	Percentage values			
			N	M + L	P + S	Recovery
min		*units*/g*				
0	Control	8.0	6.4	80.3	13.4	101.2
	Glucagon	10.0‡	7.5§	76.4§	16.1§	96.3
10	Control	8.2	3.6	79.4	17.0	104.2
	Glucagon	7.8§	4.9§	77.6§	17.6§	105.0
20	Control	13.4‖	5.2‖	76.6‖	18.2‖	92.2‖
	Glucagon	11.1	6.0	74.0	20.0	97.3
30	Control	8.6	8.4	75.3	16.4	90.8
	Glucagon	9.2§	5.7§	73.5§	21.2¶	97.3
40	Control	9.9	4.9	74.3	20.9	99.3
	Glucagon	9.7§	5.3§	72.9§	21.9§	104.1
50	Control	9.1	5.8	71.0	23.3	95.9
	Glucagon	10.4**	7.6§	67.2§	25.2§	96.8

* One unit is the amount of enzyme releasing one μmole of inorganic phosphate per minute.
‡ $P < 0.01$.
§ $P > 0.05$.
‖ Only one value available.
¶ $P < 0.02$.
** $P < 0.05$.

through the use of mathematical procedures based on the methods of Delesse (13) and Wicksell (14). A correction for the effect of section thickness, estimated from interference colors and found to average 0.074 μ, on relative volume measurements was made as described by Baudhuin (12). Characterization of the contents of autophagic vacuole profiles and their limiting membranes was made following examination of each profile in the final print with a stereoscopic microscope (American Optical Corporation, Buffalo, N.Y.) at × 7.

RESULTS

Acid Phosphatase

TOTAL ACTIVITY: The total acid phosphatase activity per gram found in livers of control and glucagon-treated animals sacrificed at various times after treatment is presented in Table I. Factorial variance analysis indicated a significant glucagon effect which was found to be due to increases at 0 and 50 min postinjection. Differences at other time points were not shown to be significant, and inspection of the data revealed that the acid phosphatase activity of glucagon-treated animals was both higher and lower than that of the control animals.

DISTRIBUTION IN FRACTIONS: The distribution of acid phosphatase in various fractions obtained by differential centrifugation is presented in Table I. Factorial variance analysis detected a glucagon effect only in P + S fractions. Evaluation of individual means indicated that glucagon caused a significant increase in the enzyme activity of this fraction only at the 30 min time point.

ACCESSIBILITY: With the homogenization and centrifugation methods used in these experiments, 81.1% of the acid phosphatase of controls remained latent, if one assumes, in the absence of

TABLE II

Effect of Homogenization and Centrifugation on the Latency of Acid Phosphatase in Control Animals

Values given in rows 1 and 2 are means ± SEM derived from 11 control animals sacrificed between 0 and 50 min postinjection. Accessible activity refers to enzyme which can be measured in fractions in the absence of detergent. Latent activity refers to that portion of the total activity which becomes measureable only after detergent addition. This activity is either assumed to be 100% (N) or is calculated by subtracting, from the percent of total activity in the fraction, that portion which is accessible (M + L, P + S).

Parameter	N	M + L	P + S
Total activity, % of N + E	5.7 ± 0.50	76.1 ± 1.22	18.2 ± 1.12
Accessible activity, % of total activity in N + E	—	7.6 ± 0.65	11.2 ± 0.75
Latent activity, % of total activity in N + E	5.7	68.5	7.0
Latent activity, normalized to 100%	7.0	84.4	8.6

actual data, that all of the activity of the N fraction is in the latent form (Table II). 84.4% of this latent activity was found in the M + L fraction with approximately equal amounts in the N and P + S fractions. Reconstruction of an average cytoplasmic extract from values for the average M + L and P + S fractions gave a latency of 81.1%. 83.3% was found by direct measurement.

The effect of glucagon treatment and osmotic shock on the accessibility of acid phosphatase in various fractions is given in Table III. Factoral variance analysis indicated that there was a glucagon or osmotic effect only in the E and M + L fractions. Prior to osmotic shock, significant increases in accessible enzyme activity were found at 30 min in the E fractions and at 40 min in the M + L fractions of glucagon-treated animals. Osmotic shock caused increases in accessible enzyme activity at all time points in E and M + L fractions from both control and treated animals. Beginning at 40 min in cytoplasmic extracts and 30 min in M + L fractions, a statistically detectable enhancement of this osmotic effect was found after glucagon treatment. As shown in Fig. 1 *a* for M + L fractions, this increased sensitivity to osmotic shock begins between 10 and 20 min postinjection and appears to be reaching a plateau by 50 min. A similar time course was observed with cytoplasmic extracts but the changes were less pronounced.

Dense Bodies

CONTROLS: Morphometric analyses of dense body populations found in M + L fractions taken from the livers of 12 control animals are summarized in Table IV and Fig. 2. The values for particle parameters obtained from pooled profile size distributions are also given in Table IV and do not deviate significantly from average values. Comparison of these results with those obtained by Deter et al. (3) and Baudhuin (12) indicate that the dense bodies studied in these investigations have a somewhat smaller mean volume, are less numerous, and constitute a lesser fraction of the liver volume. The latter parameter has a value which is only 48.5% of that obtained by Baudhuin but is underestimated due to the loss of dense bodies during homogenization and fractionation. Baudhuin has estimated this loss from enzyme measurements and has introduced a correction based on an average of the amounts of acid phosphatase (61.1 ± 1.4 SD %) and acid deoxyribonuclease (75.1 ± 5.2 SD %) found in M + L fractions. As a value for the acid deoxyribonuclease content of these M + L fractions was not available, a similar correction could be made with only acid phosphatase. Applying this correction, the fractional volume occupied by dense bodies was found to be only 60.2% of that found by Baudhuin. No explanation for this discrepancy is readily apparent but it should be noted that sex (male vs. female)

TABLE III

Effect of Glucagon on the Accessibility of Acid Phosphatase before and after Osmotic Shock

Values given are means calculated from data obtained from either two (control) or four (glucagon) animals. Results were analyzed statistically by 2 × 2 × 6 factorial variance analysis. Pairs of means at each time point were compared by *t* tests.

Time after treatment	Treatment	Accessible activity, % of total activity in fraction					
		E		M + L		P + S	
		Untreated	Osmotic shock*	Untreated	Osmotic shock*	Untreated	Osmotic shock*
min							
0	Control	16.9	28.7	7.6	21.5	84.3‡	70.8
	Glucagon	13.4§	29.7§	10.0§	18.8§	57.8	61.8
10	Control	14.7	26.1	8.2	22.1	57.3	69.1
	Glucagon	14.7§	26.9§	9.8§	23.3§	57.3	59.4
20	Control	15.7‡	23.0‡	9.0‡	21.6‡	58.8‡	54.3‡
	Glucagon	15.8	33.7	9.2	25.8	60.1	55.1
30	Control	12.1	27.8	11.9	25.9	60.5	65.0
	Glucagon	18.8‖	33.6§	13.0§	34.4¶	49.0	56.8
40	Control	16.2	32.9	12.1	30.8	57.9	62.1
	Glucagon	21.1§	49.1¶	17.9¶	49.0¶	60.4	64.3
50	Control	21.5	33.9	10.9	30.2	66.0	66.8
	Glucagon	21.5§	52.5¶	14.3§	54.8¶	62.1	65.7

* Exposed to 0.15 M sucrose for 30 min at 0°C. then brought back to 0.25 M sucrose before assay.

‡ Only one value available.

§ $P > 0.05$.

‖ $P < 0.05$.

¶ $P < 0.01$.

and strain (Sprague-Dawley vs. Wistar) differences exist in the two groups of animals studied.

As shown previously (11, 12), morphometric data of the type obtained in these experiments can be used to construct sedimentation coefficient distribution digrams which are comparable to those obtained by centrifugation for particle-bound enzymes. In Fig. 2 *b*, the cumulative sedimentation coefficient distributions for dense bodies (derived from 12 control animals), acid phosphatase and acid deoxyribonuclease (2) are presented. Construction of the distribution for dense bodies required an estimated value for unsedimentable and slow sedimenting constituents which was taken as the average of the mean acid phosphatase content of P + S fractions and the mean unsedimentable acid deoxyribonuclease, determined in previous experiments (2). This latter value was considered to be a reasonable estimator of the acid deoxyribonuclease content of the P + S in these experiments, as previous results have shown very little slow sedimenting acid deoxyribonuclease, and the use of unwashed M + L fractions would be expected to further decrease the contribution of particulate-bound enzyme to the total enzyme content of P + S fractions (compare the distribution of acid phosphatase presented here with the distributions obtained by de Duve et al. [6] and Baudhuin et al. [15]). A second correction, namely the establishment of a plateau at 0.92, was also necessary in order to make the dense body sedimentation coefficient distribution comparable to the enzyme

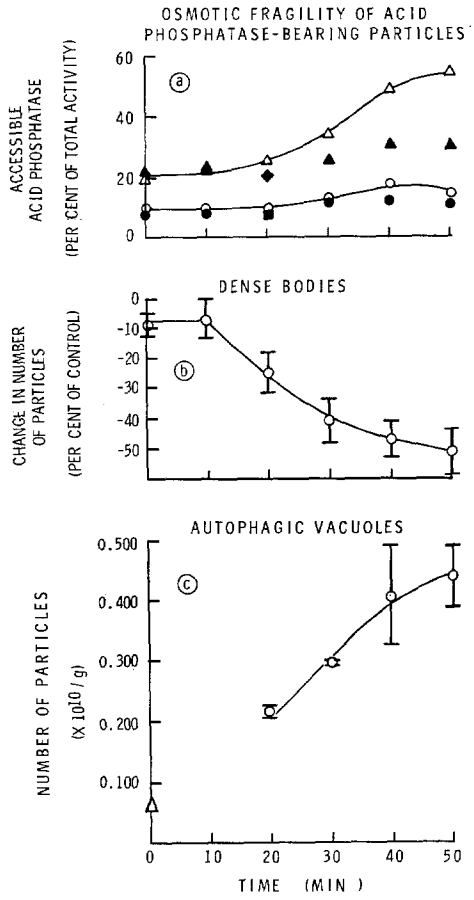

FIGURE 1 Effect of glucagon on various particle populations found in M + L fractions. In 1 *a*, accessible acid phosphatase activities of controls before (●) and after (▲) osmotic shock are given with those from glucagon-treated animals before (○) and after (△) shock. Values plotted are means calculated from data obtained from either two (controls) or four (glucagon-treated) animals. (■) and (◆) represent single control values. In 1 *b*, values plotted are means ±SEM calculated from data obtained from the two control and three glucagon-treated animals studied at each time point. In 1 *c*, means ±SEM, calculated from data obtained from the three glucagon-treated animals studied at each time point, are plotted as open circles (○). The open triangle (△) indicates a value for controls obtained by pooling data from 12 control animals.

distributions. As discussed by Deter and de Duve (2), there appears to be a certain fraction of particles containing lysosomal enzymes which sediment completely during the centrifugation process. As morphometry has failed to reveal the presence of particles which could have this sedimentation behavior, it has been suggested that these particles represent agglutinated aggregates of other enzyme-containing constituents or experimental artifact (12). As there is no evidence to indicate that all particle subclasses are not affected equally, one can treat this class as representing a random loss of enzyme-containing constituents. Baudhuin (12) has indicated that the appropriate correction of the dense body sedimentation coefficient distribution is the establishment of a plateau at a value equal to the average of the plateau values found for acid phosphatase and acid deoxyribonuclease (2). The sedimentation coefficient distribution for dense bodies obtained after these corrections are made falls between that of acid phosphatase and that of acid deoxyribonuclease, with a median sedimentation coefficient of 4.35. The average median sedimentation coefficients for acid phosphatase and acid deoxyribonuclease are 3.9 and 5.1, respectively, averaging 4.5 (2). These results indicate that the sedimentation behavior of at least 71.5% of the acid phosphatase and 70.6% of the acid deoxyribonuclease of the liver can be explained by assuming association of these two enzymes with dense bodies. A small proportion (5–10% in the case of acid phosphatase) of the enzyme activity is associated with slow sedimenting constituents which could originate from membrane systems such as the Golgi apparatus.

GLUCAGON-TREATED ANIMALS: Table V gives the average morphometric parameters of hepatic dense body populations taken from control and glucagon-treated animals at various times after injection. Factorial variance analysis revealed a significant effect of glucagon on the mean radius, the mean volume, the fractional volume, and the number of these particles. This effect appeared to depend upon the time after injection, but only in the case of the number of dense bodies was this interaction statistically significant. The effect of glucagon on dense body number can best be seen by a plot of the differences between treated animals and their associated control, expressed as per cent of the control, as shown in Fig. 1 *b*. This procedure permits a correction for differences in initial dense body number but assumes that the number of dense bodies found in the control is a good estimator of the initial number of dense bodies in the glucagon-treated animal. As shown in Fig. 1 *b*, loss of dense bodies begins between 10 and 20 min postinjection and continues

TABLE IV

Morphometric Parameters of Control Dense Body Population

Average values are those derived from 12 control animals sacrificed between 0 and 50 min postinjection. For comparison, parameters calculated from the composite profile size distribution (class interval = 0.0356 μ), obtained by pooling individual profile size distributions of all control animals, are given. The data from Baudhuin (12) are averages derived from 4 animals receiving no treatment.

Parameter	Average ± SEM	Pooled profiles	From Baudhuin (12) average ± SEM
Mean radius, μ	0.222 ±0.002	0.224	0.230 ±0.005
Meadian radius, μ	0.209 ±0.003	0.211	0.210 ±0.005
Standard deviation of radius, μ	0.061 ±0.003	0.060	0.065 ±0.004
Mean volume, μ^3	0.057 ±0.002	0.059	0.066 ±0.003
Fractional volume*, $cm^3/100\ cm^3$	0.184‡ ±0.011	0.177	0.379§ 0.007
Number per gram, $\times 10^{10}$	3.07‡ ±0.16	2.87	6.10§ ±0.002

* Fractional volume refers to the volume occupied by a particle population in a given volume of liver tissue.

‡ Uncorrected for loss during homogenization and fractionation.

§ Corrected for loss during homogenization and fractionation.

throughout the entire 50 min period studied. The rate of loss is highest initially and decreases progressively with time. Preliminary analysis indicates that the dense body decrease does not follow simple first or second order kinetics. By using the average number of dense bodies per gram determined from 12 control preparations (Table IV) and assuming a constant loss rate between adjacent time points, one can calculate dense body disappearance rates over the intervals 10–20, 20–30, 30–40, and 40–50 min, of 5.5, 4.1, 2.5, and 1.6 $\times$ 10^8/min per g, respectively. The size distributions derived from pooled dense body profiles of control and glucagon-treated animals (Fig. 3) suggest a preferential loss of small particles, except between 10 and 20 min, even though variations in the shape of the distributions exist. As discussed by Baudhuin and Berthet (11), these variations may be due in part to sampling error which is magnified by the Wicksell procedure. However, because of their origins, dense body populations in different animals are likely to vary significantly.

Decreases in the total volume occupied by dense bodies (volumes not corrected for losses due to homogenization and fractionation which appear to be comparable in almost all preparations) following glucagon administration can be calculated if one again assumes that control values are good estimators of the initial values in treated animals. On the average, these changes, expressed as per cent of control, were found to vary between 6 and 30% depending upon the time after injection. However, only the differences at 40 and 50 min could be shown to be statistically significant.

Autophagic Vacuoles

MORPHOMETRIC PARAMETERS: In Table VI the morphometric parameters of autophagic vacuole populations found in M + L fractions of rat liver taken from controls and treated animals killed at various times after treatment are presented. Both averages and values calculated from composite profile size distributions, obtained by pooling data from the three animals studied at

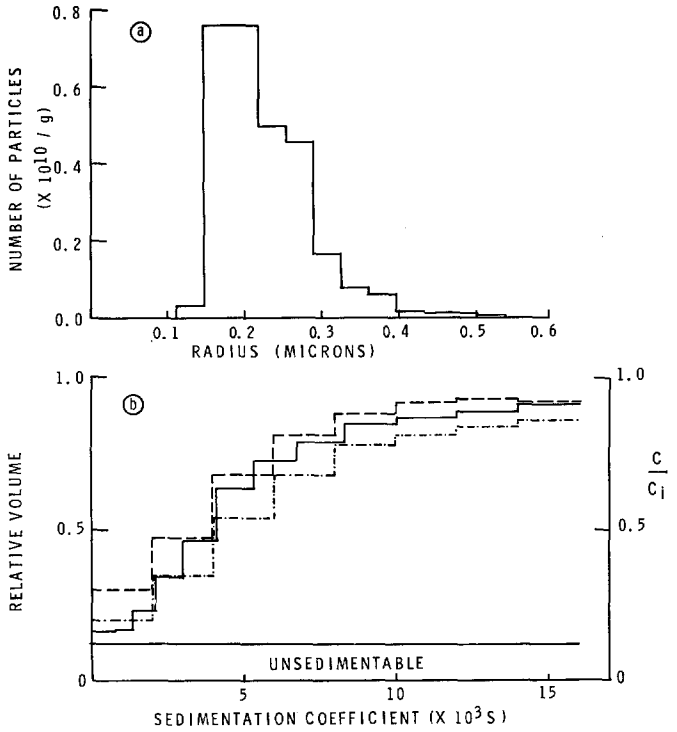

FIGURE 2 Size and cumulative sedimentation coefficient distributions for dense bodies from control animals. Results were calculated from the composite profile size distribution (class interval = 0.0356 μ), obtained by pooling individual profile size distributions from 12 control animals. In 2 b, the sedimentation coefficient distribution calculated for dense bodies (——) is plotted with the sedimentation boundaries of acid phosphatase (----) and acid deoxyribonuclease (-·-·-·-) obtained previously (2). The average of the mean unsedimentable acid phosphatase and acid deoxyribonuclease activities is indicated at the bottom of the figure. The left ordinate gives the relative volume of dense bodies, while on the right, C_i and C refer to enzyme concentrations before and after centrifugation, respectively.

each time point are given. Autophagic vacuoles are only rarely seen in control preparations, but by pooling the data from 12 animals, 55 profiles were obtained. Average mean volumes were found to be somewhat smaller than the mean volumes derived from pooled profiles, but the values for fractional volume were comparable with either method of calculation. This results in the average number of particles per gram being greater than the number of particles per gram calculated from pooled profiles. A profile sample size which is too small could be responsible for these differences. Comparison of these data with those for dense bodies given in Table IV indicates that autophagic vacuoles have, on the average, a mean volume which is 440–870% larger, occupy fractional volumes which are 10–114% of that occupied by dense bodies, and are 2–14% as numerous, depending upon the time after injection. As illustrated in Fig. 1 *c*, sufficient numbers of autophagic vacuole profiles for morphometric analysis were not found in individual preparations until 20 min after glucagon treatment. Data derived from pooled controls, however, gave approximate values for zero time. Between 20 and 50 min, the number of autophagic vacuoles showed a progressive rise with a tendency to plateau detected at 50 min. Autophagic vacuole formation rates were approximately 0.80, 1.09, and 0.32 $\times$ 10^8/min per g between adjacent time points. This change in number was accompanied by an increase in the mean volume, reaching a maximum at 40 min. A similar pattern was seen for the fractional volume occupied by autophagic vacuole populations. Statistical analysis of these data indicated that only the differences in number between 20 min and 40 or 50 min and the differences in mean volume between 20 min and 40 or 50 min are statistically significant. Changes in fractional vol-

TABLE V

Effect of Glucagon on the Morphometric Parameters of Dense Body Populations

Values are means calculated from data obtained from either two (control) or three (glucagon) animals. The class interval of individual profile size distributions was 0.0356 μ. Results were analyzed statistically by 2 × 2 × 6 factorial variance analysis. Pairs of means at each time point were compared by *t* tests.

Time after treatment	Treatment	Mean radius	Mean volume	Fractional volume	Number per gram
min		μ	μ^3	$cm^3/100\ cm^3$	$\times 10^{10}$
0	Control	0.220	0.055	0.208	3.63
	Glucagon	0.211*	0.050*	0.172*	3.32*
10	Control	0.228	0.060	0.147	2.43
	Glucagon	0.239*	0.066*	0.138*	1.98*
20	Control	0.221	0.055	0.157	2.75
	Glucagon	0.224*	0.062*	0.131*	2.05‡
30	Control	0.215	0.051	0.161	3.05
	Glucagon	0.243*	0.080§	0.151*	1.77‖
40	Control	0.224	0.060	0.195	3.10
	Glucagon	0.247*	0.082*	0.139‡	1.63‖
50	Control	0.225	0.065	0.234	3.44
	Glucagon	0.250*	0.096§	0.164‖	1.70‖

* $P > 0.05$.
§ $P < 0.05$.
‡ $P < 0.02$.
‖ $P < 0.01$.

ume are all significant except for that found between 40 and 50 min. The small number of animals in each group, the small size of the profile sample, and the heterogeneity of the particle populations examined (see succeeding section) make it difficult to demonstrate that differences are statistically significant. However, these results clearly indicate a growing autophagic vacuole population, both in number and in size, following glucagon administration.

TYPES OF AUTOPHAGIC VACUOLE PROFILES: Fig. 4 illustrates the principal types of autophagic vacuole profiles found in M + L fractions of liver from normal and glucagon-treated animals. To investigate the character of autophagic vacuole profile populations in more detail, the following classification system was devised and used to determine the proportion of vacuole profiles found in the various classes.

Type I profiles (Figs. 4 *a*, *b*) were defined as those which contain primarily endoplasmic reticulum, free ribosomes, and unstructured cytoplasm. The outer boundaries of these profiles were double membranes (Fig. 4 *a*), single membranes (Fig. 4 *b*), or not definable. Type II profiles had profiles of mitochondria as their predominate constituent (Figs. 4 *c*, *d*) although endoplasmic reticulum, ribosomes, and cytoplasmic matrix were also found (Fig. 4 *d*). Double and single membranes also formed the boundaries of these profiles, but in a significant proportion of the cases the nature of the limiting membrane could not be determined. Type III profiles were those which contained smooth membrane components in a finely granular matrix (Fig. 4 *e*) and were almost always bounded by single membranes. Type IV profiles (Fig. 4 *f*) were single-membrane bounded and contained primarily ground cytoplasm in which were embedded free ribosomes and, on occasion, membrane elements. In rare instances, profiles of other cytoplasmic constituents were found within a membrane-bounded space and these were classified as type V. The composition of autophagic vacuole profile populations with respect to these five classes is presented in Table VII. Types I and II predominated at every time point, with

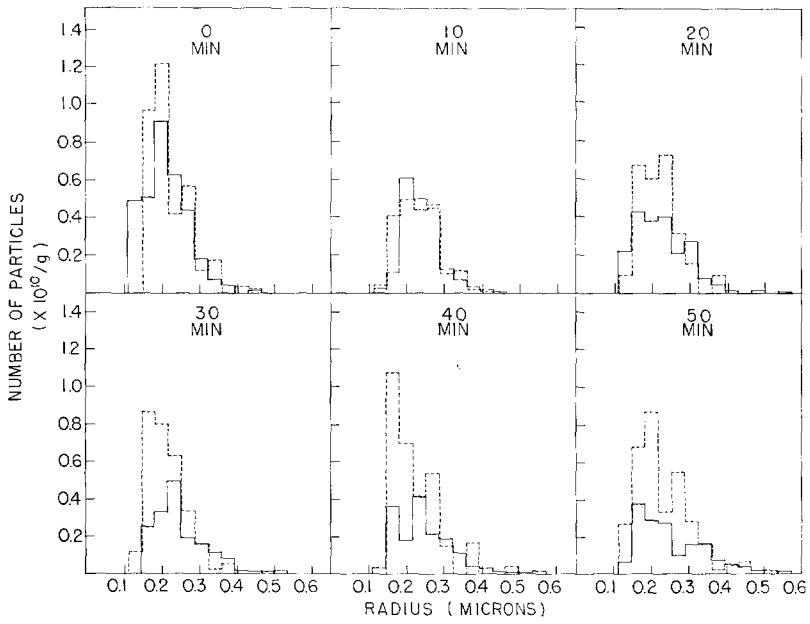

FIGURE 3 Size distributions of dense bodies in M + L fractions from control and glucagon-treated animals sacrificed at various times at treatment. Distributions for control (-----) and glucagon-treated (——) animals were calculated from composite profile size distributions (class interval = 0.0356 μ) obtained by pooling the individual profile size distributions of the three animals studied at each time point.

the proportion of type I being greater in all cases. Statistical analysis (data from controls were excluded in all statistical analyses because of the small sample size) revealed that the per cent of types I and II profiles did not differ significantly in the various autophagic vacuole profile populations except at the 20 min time point. The proportions of types III, IV, and V were not significantly different at any time point.

As types I and II represented nearly 90% of the profiles examined, it was of interest to determine the contribution of these two types to the total number of autophagic vacuoles calculated from all profiles. Profiles of each class, from the three animals examined at each time point, were pooled and the number of particles per gram was calculated as previously described. The number of particles attributable to each type was compared to the total number of particles per gram. The results of these calculations are presented in Table VII. Their validity depends upon the accuracy of classification (a type I profile might come from a type II particle if the plane of section did not pass through the sequestered mitochondrion), and on the adequacy of the sample size. The fact that the sum of the calculated number of types I and II particles exceeds the total number of autophagic vacuoles calculated from all profiles (except at 20 min), indicates an error in at least one of the parameters used in these calculations. This error is not large, however, and is probably the result of inadequate sample size.

Pooled profiles of types I and II autophagic vacuoles have also been used to calculate morphometric parameters for these two classes of vacuoles (see Table VIII). These data indicate that type II particles were consistently larger than type I particles, the ratio of mean volumes being between 1.75 and 2.36 depending upon the time after injection. The fractional volume occupied by the type I particles was initially twice that occupied by type II particles. With time there was a progressive increase in the fractional volume of both particle types, but that of the type II particles increased more rapidly, finally attaining a value which was greater than that for the type I particles. The numbers of both types of particles increased with time, but the rate of increase was again greater for type II particles except between 40 and 50 min.

TYPES OF AUTOPHAGIC VACUOLE MEMBRANES: To characterize the limiting membranes of autophagic vacuole profiles seen at various times after glucagon treatment, each pro-

TABLE VI

Morphometric Parameters of Autophagic Vacuole Populations

Average values are those derived from three glucagon-treated animals studied at each time point. The class interval of individual profile size distributions was 0.0700 μ. Variance analysis was carried out using a completely randomized design, the fractional volumes and numbers per gram requiring logarithmic transformation to achieve variance homogeneity among groups. Differences among means were evaluated by the multiple range test of Duncan. For comparison, parameters calculated from composite profile size distributions (class interval = 0.0356 μ), obtained by pooling the individual profile size distributions of the three animals studied at each time point, are given. The data for controls were obtained by pooling profiles from 12 control animals sacrificed between 0 and 50 min postinjection. The class interval for controls was 0.0700 μ.

	Averages ± SEM			Pooled profiles			
Time after glucagon administration	Mean volume	Fractional volume	Number per gram	No. of profiles	Mean volume	Fractional volume	Number per gram
min	μ^3	$cm^3/100\ cm^3$	$\times 10^{10}$		μ^3	$cm^3/100\ cm^3$	$\times 10^{10}$
Untreated control	—	—	—	55	0.250	0.018	0.068
20	0.364 ±0.010	0.082 ±0.002	0.216 ±0.011	301	0.383	0.085	0.210
30	0.404 ±0.010	0.126 ±0.005	0.296 ±0.005	305	0.406	0.114	0.268
40	0.493 ±0.034	0.209 ±0.037	0.405 ±0.081	301	0.549	0.200	0.347
50	0.415 ±0.041	0.188 ±0.016	0.437 ±0.046	303	0.465	0.193	0.395

file was examined and its membrane classified as double, single, or unknown. The results of this analysis, for total autophagic vacuole profile populations and for types I and II profile populations, are presented in Table IX. These data indicate that the predominate membrane type was the single one, regardless of the time after treatment, with approximately 50% of the profiles being bounded by single membranes and 20% by double membranes. In nearly 30% of the cases, however, the nature of the boundary could not be determined. Statistical analysis has failed to reveal any significant effect of time on the proportion of profiles having double, single, or unknown limiting membranes.

DISCUSSION

The Source of Acid Hydrolases Found in Autophagic Vacuoles after Glucagon Administration

Marked changes in the dense body, autophagic vacuole, and acid phosphatase–bearing particle populations of liver tissue following glucagon administration have again been demonstrated in this more extensive investigation of these phenomena. In previous studies (2, 3), we observed that glucagon strongly stimulated autophagic vacuole formation and initiated events which led to the loss of significant numbers of pericanalicular dense bodies. Evidence was obtained which indicated the transfer of a significant part of the lysosomal enzyme activity to particles of larger size, and autophagic vacuoles were found to have, on the average, a volume which was 4.6 times larger than that of dense bodies. These results led to the conclusion that preexisting dense bodies could be the principal source of the digestive enzymes known to exist in the autophagic vacuoles, provided they contained most of the lysosomal hydrolases found in normal liver tissue. The experiments presented here further support this conclusion by providing quantitative data which indicate an association of most of at least two lysosomal enzymes with dense bodies. The time courses of dense body loss, autophagic vacuole increase, and change in the osmotic sen-

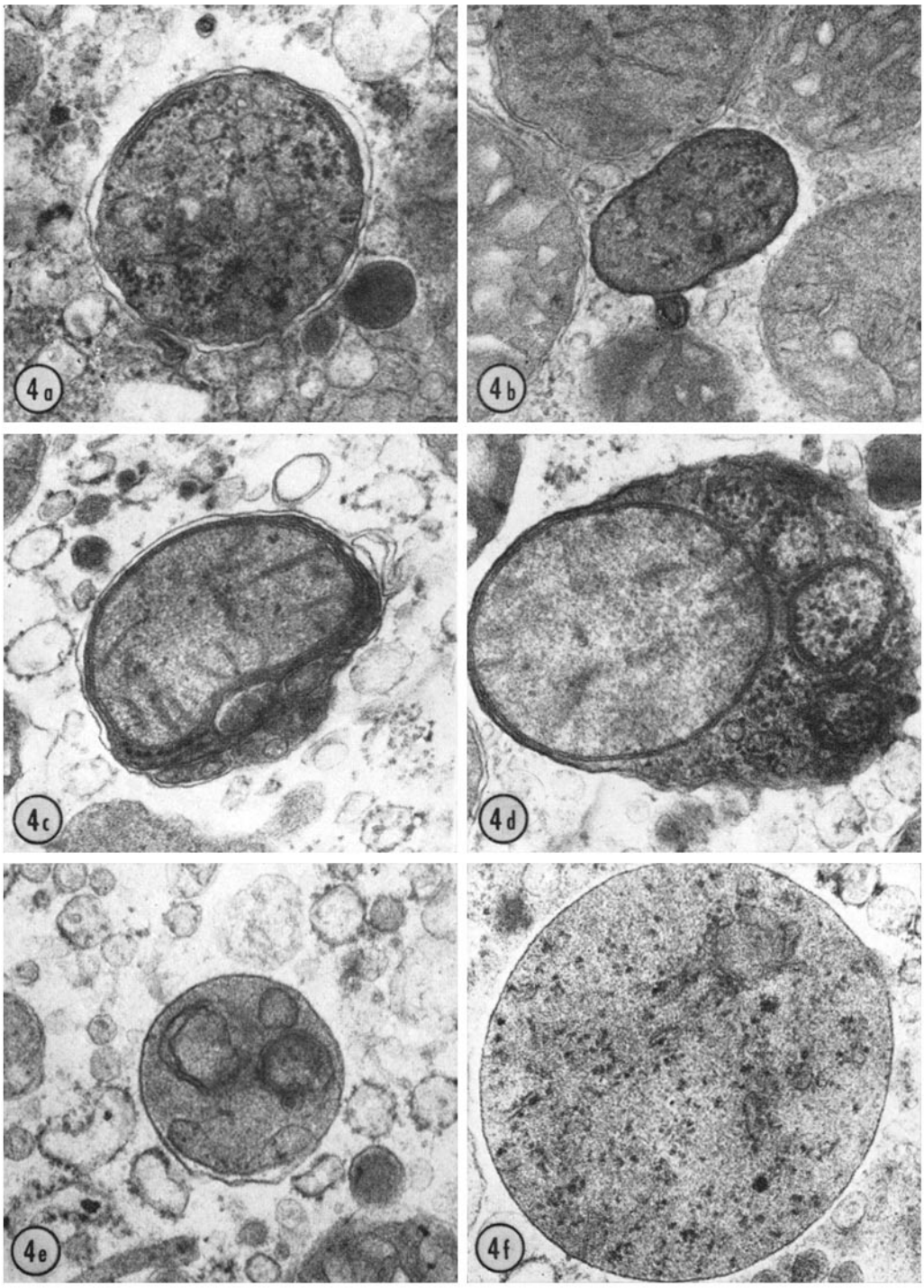

FIGURE 4 Types of autophagic vacuole profiles seen in M + L fractions from control and glucagon-treated animals. 4 *a*, Type I, double limiting membrane; 4 *b*, type I, single limiting membrane; 4 *c*, type II, double limiting membrane; 4 *d*, type II, single limiting membrane; 4 *e*, type III, single limiting membrane; 4 *f*, type IV, single limiting membrane. × 41,800.

TABLE VII

Composition of Autophagic Vacuole Populations

Values given under Profiles represent the proportions of total autophagic vacuole profile populations contributed by each of the five profile classes defined under Results. They are either means calculated from data derived from the three glucagon-treated animals studied at each time point, or individual values obtained by pooling the profiles from 12 control animals. The data from glucagon-treated animals were analyzed statistically by variance analysis, completely randomized design. Differences among means were evaluated by the multiple range test of Duncan.

The contribution of types I and II autophagic vacuoles to total autophagic vacuole particle populations is given under Particles. These data were obtained by first pooling profiles from the three glucagon-treated animals studied at each time point. The numbers of types I and II particles, as well as the total number of autophagic vacuoles, were then calculated from their respective composite profile size distributions (class interval = 0.0356 μ). The proportions of each particle type are given as percentage values.

	Profiles						Particles		
		Percentage values						Percentage values	
Time after glucagon administration	Absolute number	I	II	III	IV	V	Absolute number per gram	I	II
min							$\times 10^{10}$		
Untreated control	55	54.5	21.8	10.9	9.1	3.6	0.068	—	—
20	301	68.7	20.3	5.3	6.2	1.0	0.210	74.3	20.5
30	305	61.8	32.6	3.0	5.9	0	0.289	72.0	32.9
40	302	54.5	32.8	6.6	4.7	0.3	0.347	64.6	38.0
50	303	56.0	33.1	4.2	2.7	0.3	0.395	67.1	34.8

TABLE VIII

Morphometric Parameters of Types I and II Autophagic Vacuole Populations

Values given are those calculated from composite profile size distributions (class interval = 0.0356 μ) obtained by pooling the profiles of a given class found in preparations from the three glucagon-treated animals studied at each time point.

Time after glucagon administration	Type I				Type II			
	No. of profiles	Mean volume	Fractional volume	Number per gram	No. of profiles	Mean volume	Fractional volume	Number per gram
min		μ^3	$cm^3/100\ cm^3$	$\times 10^{10}$		μ^3	$cm^3/100\ cm^3$	$\times 10^{10}$
20	204	0.308	0.051	0.156	62	0.540	0.024	0.043
30	191	0.285	0.055	0.183	100	0.590	0.053	0.086
40	166	0.365	0.086	0.224	99	0.696	0.096	0.132
50	171	0.288	0.080	0.264	101	0.683	0.07	0.135

sitivity of acid phosphatase–bearing particles have been shown to be consistent with the hypothesis of enzyme transfer from dense bodies to autophagic vacuoles.

The biochemical studies presented in Table II indicate that a majority of the acid phosphatase–containing particles of normal liver survive homogenization and fractionation and can be found in the M + L fraction. The sedimentation behavior of acid phosphatase and other lysosomal enzymes of cytoplasmic extracts has recently been investigated and their sedimentation coefficient distributions determined (2). The quantitative morphological methods which were used in the present investigations have permitted calculation of a sedimentation coefficient distribution for the dense bodies of the M + L fraction. With certain corrections, this distribution is comparable to the distri-

TABLE IX

Limiting Membranes of Autophagic Vacuole Profiles

Values presented are means calculated from data obtained from 12 control animals or from the three glucagon-treated animals studied at each time point. They represent the proportions of the total autophagic vacuole profile populations which were assignable to each of the three membrane categories. Results, except those for controls, were analyzed statistically by variance analysis, completely randomized design. Differences among means were evaluated by the multiple range test of Duncan.

	Percentage values								
	Double			Single			Unknown		
Time after glucagon administration	All profiles	Type I	Type II	All profiles	Type I	Type II	All profiles	Type I	Type II
min									
Untreated control	18.2	—	—	67.3	—	—	14.5	—	—
20	20.7	24.6	25.5	56.0	46.7	50.4	26.0	25.3	35.9
30	24.3	31.7	13.3	51.4	41.9	56.6	27.2	32.4	29.6
40	18.7	21.8	19.7	51.3	49.2	63.8	25.6	21.3	28.8
50	16.7	19.7	18.0	48.4	54.5	54.5	30.2	27.5	26.4

butions obtained for lysosomal enzymes. As seen in Fig. 2 *b*, the dense body distribution parallels the distributions for acid phosphatase and acid deoxyribonuclease, indicating that the sedimentation behavior of these two lysosomal enzymes can be explained by assuming their association with dense bodies. These results are strong quantitative, though circumstantial, evidence that most of the acid phosphatase and acid deoxyribonuclease of normal liver tissue is located in dense bodies.

The conclusion that most of the acid phosphatase in the normal rat liver is located in pericanalicular dense bodies permits correlation of the biochemical and morphometric data presented in Fig. 1. The loss of dense bodies following glucagon treatment correlates well with the increase in osmotic fragility of acid phosphatase-bearing particles, as would be expected if enzymes were being transferred to particles more sensitive to osmotic shock. The loss of dense body volume (between 6 and 30%, depending on the time after treatment) is sufficient to explain the increased accessibility of acid phosphatase (between 4 and 21%). The alternatives to enzyme redistribution are new enzyme synthesis, with subsequent transfer to osmotically sensitive particles, or sensitization of the membranes of remaining dense bodies to osmotic shock. The former has not been found consistently in these experiments (Table I), and was not found in three other investigations (2–4). Although there is no evidence to exclude the latter, previous studies (2) have shown that acid phosphatase is transferred to particles of larger size which would be expected to be more sensitive to osmotic shock. The presence of increasing numbers of autophagic vacuoles during the period of dense body loss and increase in the osmotic fragility of acid phosphatase-bearing particles, together with the large size of these vacuoles and their acid phosphatse positivity (4), suggests that transfer of lysosomal enzymes from dense bodies to autophagic vacuoles is a more plausible explanation for the observations which have been made. Direct evidence that such a transfer can occur under these conditions has recently been provided by Ericsson (5).

A different source for the lysosomal hydrolases found in autophagic vacuoles which develop after glucagon administration has recently been postulated by Arstila and Trump (4). These investigators concluded that, while secondary lysosomes (i.e. dense bodies) may contribute to a limited extent, Golgi vesicles provide most of the lysosomal enzymes of autophagic vacuoles for the following reasons: (*a*) The lysosomal hydrolases of autophagic vacuoles can also be found in Golgi vesicles by cytochemical techniques. (*b*) The double-walled sacs forming the boundary of autophagic vacuoles frequently have at least one membrane of a thicker size class which is characteristic of lysosomes. (*c*) Preloading of secondary lysosomes with ferritin or polyvinylpyrrolidone prior to glucagon treatment results in only limited mixing of the contents of these secondary lysosomes and with the contents of autophagic vacuoles. (*d*) Autophagic vacuoles ordinarily occur in the vicinity of the Golgi apparatus. (*e*) Images suggestive of fusion between the double-walled sacs bounding autophagic vacuoles and the mem-

branes of Golgi vesicles have been seen. On close inspection, however, these observations do not appear to be sufficient to support this concept. Observations (*a*) and (*b*) are not specific for Golgi vesicles and apply equally to secondary lysosomes (dense bodies). With respect to observation (*c*), Ericsson (5) has reached the opposite conclusion in a similar study of glucagon-induced autophagy in animals whose secondary lysosomes were preloaded with an iron–sorbitol–citric acid complex. Observation (*d*) seems questionable in view of the contradictory interpretation of these data given in the discussion of the origin of autophagic vacuole membranes from elements of the smooth endoplasmic reticulum (see p. 703 of reference 4). With respect to observation (*e*), it appears doubtful that a dynamic process such as vacuole fusion can be adequately evaluated from static electron micrographs whose representativeness is unknown. In the electron microscope, vacuole fission or simple juxtaposition of vacuoles would be difficult to distinguish from vacuole fusion.

The data of Arstila and Trump (5), however, do provide evidence for dense bodies as the source of the lysosomal hydrolases of autophagic vacuoles. These authors have submitted M + L fractions of liver, taken from normal and glucagon-treated animals, to glycogen-sucrose density gradient centrifugation and have determined the distribution of acid phosphatase in these gradients. The results indicate that, following glucagon, most of the acid phosphatase is found in particles having densities greater or lesser than those which characterize the particles containing the enzyme in normal animals. These results were interpreted as indicating a transfer of enzyme from Golgi vesicles to autophagic vacuoles, a conclusion based on an estimate of the contribution of the Golgi apparatus to the total acid phosphatase activity of possibly as much as 50%, made from qualitative cytochemical observations. The actual Golgi vesicle content of the fractions submitted to density gradient centrifugation is unknown, however, as no quantitative morphological or biochemical evaluation was made. Recent investigations have indicated that the sedimentation properties of Golgi constituents are very dependent upon the method of homogenization. Gentle homogenization (16) results in intact Golgi apparatuses which can be sedimented with low centrifugal forces (44,000 $g \times$ min). Homogenization procedures (17, 18) similar to those of Arstila and Trump cause fragmentation, and high centrifugal forces (between 250,000 and 1,000,000 $g \times$ min) are needed to sediment Golgi derivatives. The fractions used by Arstila and Trump in gradient experiments were obtained under conditions (between 10,000 and 250,000 $g \times$ min) which are intermediate to those used by other investigators for the isolation of Golgi apparatus constituents. In view of the unknown contribution of the Golgi apparatus to the acid phosphatase of these fractions, and the evidence indicating that this enzyme is primarily located in dense bodies, it seems likely that the changes in the acid phosphatase distribution seen by Arstila and Trump following glucagon administration indicate transfer of enzyme from dense bodies rather than from constituents of the Golgi apparatus. The presence of the enzyme in denser and lighter particles may provide an explanation, in part at least, for the sedimentation behavior of acid phosphatase–bearing particles in cytoplasmic extracts from livers of glucagon-treated animals (2).

The Sequestration of Cytoplasmic Constituents after Glucagon Administration

The autophagic vacuole populations found in these investigations approximate those which might have been expected from a segregation process operating in a cytoplasm where 74.3% of the volume is occupied by ground substance and endoplasmic reticulum, and 23.0% by mitochondria (19); this assumes that autophagic vacuoles can be formed, with equal probability, in all parts of the cytoplasm. If the volumes of cytoplasmic constituents within vacuoles do not change, at least 0.027–0.259% of the cytoplasmic volume would be sequestered, depending upon the time after the injection of glucagon. However, the definitive character of the autophagic vacuole-cytoplasm relationship is not known, though certain observations may be relevant. Of particular interest is the conspicuous absence of profiles of peroxisomes and dense bodies in sectioned autophagic vacuoles. These constituents represent only a very small per cent of the cytoplasmic volume in intact tissue, 1.5 and 0.9% respectively (19), but but they could have been found if their fractional volume within autophagic vacuoles was similar to their fractional volume in the cytoplasm. In an autophagic vacuole profile area of 697.0 μ^2, the peroxisome population would be expected to give profiles with an area of 10.5 μ^2. Using the data of

Weibel et al. (19), one can calculate that this area would represent 26.5 equatorial profiles having radii of 0.355 μ (the radius of a peroxisome having an average volume of 0.187 μ^3, assuming sphericity). Allowing nonequatorial profiles or using the radius of 0.265 μ found for peroxisomes in M + L fractions by Baudhuin (12), one would expect an even larger number of profiles. As only one definite peroxisome profile was seen, these particles must be specifically excluded during the segregation process unless (*a*) rapid disintegration occurs after entering autophagic vacuoles, (*b*) incorporation occurs by membrane fusion, (*c*) vacuoles containing these particles are specifically lost during the preparation procedure, or (*d*) the sample studied is highly unrepresentative. Similar calculations indicate that 40.5 dense body profiles should have been found though only two were actually observed. The absence of dense body profiles might also be interpreted as indicating a specific particle exclusion, although rapid breakdown cannot be excluded. The observation of Arstila and Trump (4) that acid phosphatase appears in the space between the limiting membranes of autophagic vacuoles suggests that membrane fusion is a mechanism by which dense body constituents could enter autophagic vacuoles.

Regardless of the basis for their segregation, all cytoplasmic elements appear to be sequestered within vacuoles having smooth membranes, either single or double in character. No evidence was obtained to indicate any involvement of the rough endoplasmic reticulum. Support for the concept of transition from double membrane-bounded to single membrane-bounded vacuoles was not obtained in these experiments. Individual variation, the inability to determine the type of membrane in a significant number of instances, and difficulties in evaluating the effects of homogenization and centrifugation make detection of a process of this type rather unlikely. The contents of most autophagic vacuoles studied appeared to be relatively normal, but in one preparation at 50 min, particles having a disorganized structure were seen. This observation, together with the diminishing rates of dense body loss, autophagic vacuole formation, and increase in the osmotic sensitivity of acid phosphatase–bearing particles, suggests that, after 50 min, digestion of sequestered material may predominate over formation of new vacuoles and interaction with dense bodies. Quantitative characterization of this phase of the autophagic process induced by glucagon remains for future investigations.

The author would like to express his sincere appreciation to Mrs. Velma Caldwell and Miss Cynthia Kronenberger for their excellent technical assistance, to Dr. E. J. Wheeler for his valuable advice and suggestions, and to Dr. O. K. Behrens of the Lilly Research Laboratories, Indianapolis, Indiana for his generous gift of glucagon.

These investigations were supported by a grant from the National Science Foundation (No. GB-8411). Computer services were provided by the Common Research Computer Facility, supported in part by the United States Public Health Service (No. FR 00254) and the Institute of Computer Science, supported in part by the National Institutes of Health (No. RR 259).

Received for publication 13 May 1970, and in revised form 11 August 1970.

REFERENCES

1. Ericsson, J. L. E. 1969. Mechanism of cellular autophagy. *In* Lysosomes in Biology and Pathology. J. T. Dingle and H. B. Fell, editors. American Elsevier, New York. 345.
2. Deter, R. L., and C. de Duve. 1957. Influence of glucagon, an inducer of cellular autophagy, on some physical properties of rat liver lysosomes. *J, Cell. Biol.* **33**:437.
3. Deter, R. L., P. Baudhuin, and C. de Duve. 1967. Participation of lysosomes in cellular autophagy induced in rat liver by glucagon. *J. Cell Biol.* **35**:C11.
4. Arstila, A. U., and B. J. Trump. 1968. Studies on cellular autophagocytosis. The formation of autophagic vacuoles in the liver after glucagon administration. *Amer. J. Pathol.* **53**:687.
5. Ericsson, J. L. E. 1969. Studies on induced cellular autophagy I. Electron microscopy of cells with in vivo labelled lysosomes. *Exp. Cell Res.* **55**:95.
6. de Duve, C., B. C. Pressman, R. Gianetto, R. Wattiaux, and F. Appelmans. 1955. Tissue Fractionation Studies. 6. Intracellular distribution patterns of enzymes in rat liver tissue. *Biochem. J.* **60**:604.
7. Baudhuin, P., P. Evrard, and J. Berthet. 1967. Electron microscopic examination of subcellular fractions I. Preparation of representative samples from suspensions of particles. *J. Cell Biol.* **32**:181.
8. Frasca, J. M. and V. R. Parks. 1965. A routine technique for double-staining ultrathin sections using uranyl and lead salts. *J. Cell Biol.* **25**:157.

9. VENABLE, J. H. and R. COGGESHALL. 1965. A simplified lead citrate stain for use in electron microscopy. *J. Cell Biol.* **25**:407.
10. TONAKI, H., J. HANACEK, and WILLIAM BLOOM. 1968. A 70 mm roll-film camera for electron microscopes. *Sci. Instrum. (News)* **13**(2): 10.
11. BAUDHUIN, P. and J. BERTHET. 1967. Electron microscopic examination of subcellular fractions. II. Quantitative analysis of the mitochondrial population isolated from rat liver. *J. Cell Biol.* **35**:631.
12. BAUDHUIN, P. 1968. L'ànalyse morphologique quantitative de fractions subcellulaires. Thése. Universite de Louvain, Louvain, Belgium.
13. DELESSE, A. 1847. Procédé mécanique pour determiner la composition des roches. *C.R.H. Acad. Sci.* **25**:544.
14. WICKSELL, S. D. 1925. The corpuscle problem: A mathematical study of a biometric problem. *Biometrika Cambr.* **17**:84.
15. BAUDHUIN, P., H. BEAUFAY, Y. RAHMAN-LI, O. Z. SELLINGER, R. WATTIAUX, P. JACQUES, and C. DE DUVE. 1964. Tissue fractionation studies. 17. Intracellular distribution of monoamine oxidase, aspartate amino-transferase, alanine aminotransferase, D-amino acid oxidase and catalase in rat liver tissue. *Biochem. J.* **92**:179.
16. MORRÉ D. J., R. L. HAMILTON, H. H. MOLLENHAUER, R. W. MAHLEY, W. P. CUNNINGHAM, R. D. CHEETHAM, and V. S. LEQUIRE. 1970. Isolation of a Golgi apparatus-rich fraction from rat liver. I. Method and morphology. *J. Cell Biol.* **44**:484.
17. MORRÉ, D. J. and H. H. MOLLENHAUER. 1964. Isolation of the Golgi apparatus from plant cells. *J. Cell Biol.* **23**:295.
18. FLEISCHER, B., S. FLEISCHER, and H. OZAWA. 1969. Isolation and characterization of Golgi membranes from bovine liver. *J. Cell Biol.* **43**:59.
19. WEIBEL, W. R., W. STÄUBLI, H. R. GNÄGI, and F. A. HESS. 1969. Correlated morphometric and biochemical studies of the liver cell. I. Morphometric model, stereologic methods and normal morphometric data from rat liver. *J. Cell Biol.* **42**:68.
20. ERICSSON, J. L. E. 1969. Studies on induced cellular autophagy. II. Characterization of the membranes bordering autophagosomes in parenchymal liver cells. *Exp. Cell Res.* **56**:393.